Roles of Surface Heterogeneity and Lateral Interactions on the Isosteric Heat of Adsorption and Adsorbed Phase Heat Capacity

Shaheen A. Al-Muhtaseb and James A. Ritter*

Department of Chemical Engineering, Swearingen Engineering Center, University of South Carolina, Columbia, South Carolina 29208

Received: October 21, 1998; In Final Form: January 26, 1999

Analytical expressions are developed, based on a lattice statistics model incorporating the Bragg−Williams approximation and a random heterogeneous surface described by a uniform distribution of energies, for predicting the single-component isosteric heat of adsorption and differential adsorbed phase heat capacity as a function of temperature, surface coverage, lateral interactions, and adsorbent heterogeneity. A parametric study demonstrates that these four factors all affect the isosteric heat of adsorption but with different magnitudes at different conditions. The temperature dependence of the isosteric heat of adsorption is always related to, and accompanied by, the adsorbent surface heterogeneity. The differential adsorbed phase heat capacity has a very weak temperature dependence and is not directly affected by lateral interactions. The molar adsorbed phase heat capacity is in most cases higher than the gas phase heat capacity. The deviation between the molar adsorbed and gas phase heat capacities depend mostly on surface coverage and surface heterogeneity and weakly on the lateral interactions and temperature. The derived expressions are used also to predict the isosteric heat of adsorption and adsorbed phase heat capacity from regressed parameters obtained from experimental adsorption isotherm data in the literature. Comparisons show that the molar adsorbed phase heat capacity can sometimes exceed it by 20% or more, depending on the regressed value of the heterogeneity parameter. These results have significant implications for adsorption-process modeling.

Introduction

The effects of surface heterogeneity and lateral interactions on adsorption equilibria have been analyzed extensively in the literature, both experimentally and theoretically.[1−5] However, these same effects on the isosteric heat of adsorption have been discussed only on the bases of experimental data with essentially no theoretical analyses to quantify their roles.[5] Recent literature has demonstrated also the importance of the potential effects of temperature on the isosteric heat of adsorption[6,7] based on thermodynamically consistent virial-type and modified Antoine adsorption models. However, a paucity of theoretical analyses have been performed demonstrating the coupled effects of temperature, surface heterogeneity, and lateral interactions on the isosteric heat of adsorption and its temperature dependence which leads to the adsorbed phase heat capacity.[8,9]

The results from a molecular dynamics (MD) simulation of the adsorption of *p*-xylene on a Na−Y zeolite[8] demonstrated that the heat of adsorption has essentially the same temperature dependence as the adsorbate−adsorbent vertical interactions and that the adsorbate−adsorbate lateral interactions are almost temperature-independent. The adsorbate−adsorbate lateral interactions also have much less contribution to the heat of adsorption than the adsorbate−adsorbent lateral interactions. A statistical mechanics study[9] employing the McQuistan−Hock model demonstrated that the adsorbed phase heat capacity of rare gases on graphite depends on the fractional surface coverage and temperature. This model contains the effects of interactions between the adsorbate molecules and the adsorbent, between two nearest-neighbor vacant sites, and between two nearest-neighbor occupied sites; however, it does not discriminate clearly between the effects of these different types of interactions, and it does not account for adsorbent heterogeneity. Moreover, these molecular simulation approaches, although elegant, are very computer intensive and, thus, not well suited for carrying out extensive parametric studies. In contrast, lattice gas concepts[10,11] have been used widely by many investigators to disclose subtle information about the adsorption of gases and their mixtures largely based on analytical expressions.[12]

These lattice-gas analyses, in many cases, have been based on a random heterogeneous surface with the lateral interactions being accounted using the Bragg−Williams approximation, mainly because these two assumptions have led to simple expressions that capture the physical essence of more realistic models. These studies have included the effects of adsorbent heterogeneity and lateral interactions on adsorption equilibria, and the roles of different energetic site distributions.[4−5,12−24] For example, Ritter et al.[4] developed an analytical expression to describe the adsorption of single gases that laterally interact on a random heterogeneous surface according to the Bragg−Williams approximation and a uniform distribution of energies. The foundation of this model is based on the rigorous theory of Hill[10] but is obtained using a method proposed by Jaroniec and Patrykiejew.[16] This adsorption isotherm model is explicit also in pressure and thus ideally suited for obtaining an explicit, analytical temperature-dependent expression for the isosteric heat of adsorption and related thermodynamic properties. Therefore, Ritter et al.'s[4] model is used herein to derive expressions for the isosteric heat of adsorption and the differential adsorbed phase heat capacity, both as functions of the fractional-surface coverage, temperature, lateral interactions, and adsorbent surface heterogeneity.

* To whom correspondence should be addressed. Phone: (803) 777−3590. Fax: (803) 777−8265. E-mail: ritter@sun.che.sc.edu.

10.1021/jp984110s CCC: $18.00
Published on Web 03/13/1999

A parametric study is performed using these new expressions to investigate the coupled effects of these parameters on the adsorption equilibria, isosteric heat of adsorption, and adsorbed phase heat capacity. Single-component adsorption-isotherm data from the literature are correlated also with Ritter et al.'s[4] model. The corresponding isotherm parameters are used in the derived expressions to predict the isosteric heat of adsorption and, from its temperature dependence, the adsorbed phase heat capacity. The isosteric heats of adsorption predicted in this straightforward fashion are compared also with those obtained by the classical less direct approach,[25] which depends on loading-explicit adsorption-isotherm models, the chain rule to convert derivatives, and numerical differentiation.[26,27]

Theory

Ritter et al.[4] used the random heterogeneous surface concept of Hill[10] with a uniform distribution of energies to model single-component adsorption equilibria, with the Bragg−Williams approximation applied globally to account for nearest neighbor interactions. This model is expressed as

$$\theta = \frac{n}{m} = \frac{1}{2s}\ln\left(\frac{1 + Pb\exp(s)\exp(-\alpha)}{1 + Pb\exp(-s)\exp(-\alpha)}\right) \tag{1}$$

where θ and n are the fractional surface coverage and amount adsorbed on the random heterogeneous surface, respectively, m is the monolayer saturation limit, P is the gas-phase pressure, b is related to the average energy of adsorption, s is the heterogeneity term, and α is the lateral interaction term. s, α, and b are defined as

$$s = \sqrt{3}\,\frac{\sigma}{RT} \tag{2}$$

$$\alpha = \frac{z\omega}{\kappa T}\,\theta \tag{3}$$

$$b = b_0 \exp\left(\frac{\epsilon}{RT}\right) \tag{4}$$

where σ is the adsorbent surface heterogeneity, z is the fixed coordination number, ω is the lateral interaction energy (favorable when negative), ϵ is the average energy of adsorption, T is the absolute temperature, R is the universal gas constant, and κ is Boltzmann's constant. However, because of α, eq 1 is implicit in surface coverage and requires an iterative solution. On the other hand, it can be rearranged into a pressure explicit isotherm as

$$P = \frac{1}{b}\left(\frac{\exp(-s)\exp\left(\frac{z\omega}{\kappa T}\theta\right)[\exp(2s\theta) - 1]}{1 - \exp(2s\theta)\exp(-2s)}\right) \tag{5}$$

The advantage of eq 5 is that it can be used to predict thermodynamic properties that are based on pressure-explicit isotherm models such as the isosteric heat of adsorption.

Assuming ideal gas-phase behavior and a negligible adsorbed phase volume with respect to the gas-phase volume, the isosteric heat of adsorption, q, can be calculated from the Clausius−Clapeyron equation[26−28] according to

$$q = RT^2\left(\frac{\partial \ln P}{\partial T}\right)_\theta \tag{6}$$

with the surface coverage replacing the amount adsorbed, n.[29,30] Applying this formula to eqs 2−5 results in eq 7, an explicit expression for the isosteric heat of adsorption as a function of surface coverage, adsorbent surface heterogeneity, lateral interactions, and temperature.

$$q = \epsilon - R\left(\frac{z\omega}{\kappa}\right)\theta + sRT\left(1 + \frac{2\exp(-2s)\exp(2s\theta)(1-\theta)}{1 - \exp(-2s)\exp(2s\theta)} + \frac{2\theta\exp(2s\theta)}{1 - \exp(2s\theta)}\right) \tag{7}$$

In the limit as $\theta \to 0$, eq 7 reduces to

$$q^0 = \lim_{\theta\to 0} q = \epsilon + RT\left(\frac{s[1 + \exp(2s)]}{\exp(2s) - 1} - 1\right) \tag{8}$$

which is the zero-surface coverage isosteric heat of adsorption.

The *differential* adsorbed phase heat capacity, $\bar{C}_{p_a}$, is defined as the temperature derivative of the differential adsorbed phase enthalpy at constant loading, i.e.,

$$\bar{C}_{p_a} = \left(\frac{\partial \bar{H}_a}{\partial T}\right)_n \tag{9}$$

The thermodynamic definition of the isosteric heat of adsorption is the difference between the molar gas-phase enthalpy and the differential adsorbed phase enthalpy,[25] i.e.,

$$q = \tilde{H}_g - \bar{H}_a \tag{10}$$

With this definition, eq 9 can be rewritten as

$$C_{p_a} = \left(\frac{\partial \tilde{H}_g}{\partial T}\right) - \left(\frac{\partial q}{\partial T}\right)_n = \tilde{C}_{p_g} - \left(\frac{\partial q}{\partial T}\right)_\theta \tag{11}$$

where $\tilde{C}_{p_g}$ is the molar heat capacity of the gas phase at constant pressure. Applying eq 11 to eq 7 gives

$$\Delta\bar{C}_{p_a} = \bar{C}_{p_a} - \tilde{C}_{p_g} = -\left(\frac{\partial q}{\partial T}\right)_\theta \tag{12a}$$

$$= -4Rs^2\exp[2s(\theta-1)](\theta[\exp(2s\theta) - \exp[s(2\theta-1)] + \exp(s) - 1] + 1 - \exp(2s\theta))(\theta[\exp(2s\theta) + \exp[s(2\theta-1)] - \exp(s) - 1] + 1 - \exp(2s\theta))/[\exp[2s(2\theta-1)] - \exp[2s(\theta-1)] - \exp(2s\theta) + 1]^2 \tag{12b}$$

which is an explicit expression for the difference between the differential adsorbed phase and molar gas phase heat capacities and depends on the adsorbent surface heterogeneity, fractional surface coverage, and temperature but not lateral interactions. In the limit as $\theta \to 0$, eq 12b reduces to

$$\Delta\bar{C}_{p_a}{}^0 = \lim_{\theta\to 0}(\Delta\bar{C}_{p_a}) = 1 - \frac{4Rs^2\exp(2s)}{[\exp(2s) - 1]^2} \tag{13}$$

which is the zero-surface coverage difference between the differential adsorbed phase and molar gas phase heat capacities.

The molar adsorbed phase heat capacity is calculated from the molar enthalpy of the adsorbed phase using the following formula

$$\tilde{C}_{pa} = \left(\frac{\partial \tilde{H}_a}{\partial T}\right)_n = \left(\frac{\partial(\tilde{H}_g - \Delta\tilde{H}_a)}{\partial T}\right)_n = \tilde{C}p_g - \left(\frac{\partial \Delta\tilde{H}_a}{\partial T}\right)_n \tag{14a}$$

where $\Delta\tilde{H}_a$ is the difference between the molar enthalpies of

TABLE 1: Parameter Values and Ranges Investigated in the Parametric Studies

parameter	units	case A	case B	case C	case D	case E	case F
$z\omega/\kappa$	K	−1086 to +1086	−1086 to +1086	−1086 to +1086	−1086 to +1086	−1086 to +1086	
σ	kJ/mol	10^{-10}	5	15	10^{-10} to 15	10^{-10} to 10	3 to 15
ϵ	kJ/mol	20	20	20	20	20	20
b_0	MPa^{-1}	0.345	0.345	0.345	0.345	0.345	0.345

the gas and adsorbed phases and is given by[25]

$$\Delta\tilde{H}_a = \frac{1}{n}\left(\int_0^n q\,\partial n - \Pi A\right) \tag{14b}$$

and ΠA is the total spreading pressure given by[25]

$$\Pi A = RT\int_0^n \frac{\partial \ln P}{\partial \ln n}\,\partial n \tag{14c}$$

Substituting eqs 14b and 14c into eq 14a, and rearranging the resulting equation, gives the following expression for calculating the difference between the molar adsorbed and gas-phase heat capacities

$$\Delta\tilde{C}_{p_a} = \tilde{C}_{p_a} - \tilde{C}_{p_g} = \frac{1}{n}\int_0^n \left(\Delta\bar{C}_{p_a} + R\left(\frac{\partial\left[\ln P + \frac{q}{RT}\right]}{\partial \ln n}\right)_T\right)\partial n \tag{15}$$

The integral in eq 15 is evaluated numerically from the loading dependence of eqs 5, 7, and 12.

Results and Discussion

The expressions derived in this work (i.e., eqs 7 and 12), based on simple lattice statistics, have all of the features necessary to account for the effects of fractional-surface coverage, surface heterogeneity, lateral interactions, and temperature on the isosteric heat of adsorption and adsorbed phase heat capacity. Eq 7 demonstrates that the isosteric heat of adsorption depends explicitly on all four parameters, while eq 12 demonstrates that the differential adsorbed phase heat capacity only depends explicitly on three of them, namely, fractional surface coverage, adsorbent heterogeneity, and temperature; it does not depend on lateral interactions. The molar adsorbed phase heat capacity, however, depends weakly on lateral interactions through the spreading pressure term in eq 14a. These are very interesting results that have also been corroborated in the literature based on rigorous MD simulations[8] that revealed the relative temperature dependencies of different components of the heat of adsorption. Results from ref 8 for *p*-xylene adsorbed by Na−Y zeolite are plotted in Figure 1 in terms of the energy of adsorption (U) and the vertical (U_v) and lateral (U_l) interaction energies, all as functions of temperature (note that U is the sum of U_v and U_l). The temperature derivative of the adsorbent−adsorbate vertical interactions is more than 20 times that of the adsorbate−adsorbate lateral interactions; therefore, the temperature derivative of the energy of adsorption is nearly equal to that of the adsorbate−adsorbent vertical interactions, which arises mainly from adsorbent surface heterogeneity. This also makes the temperature derivative essentially independent of lateral interactions, in agreement with eq 12.

The roles of surface heterogeneity and lateral interactions on the isosteric heat of adsorption, adsorbed phase heat capacity, and adsorption equilibria at different temperatures as well as the effect of fractional surface coverage are ascertained from a parametric study. However, since the effects of these parameters on the adsorption equilibria have been studied previously,[4] more emphasis is placed here on the isosteric heat of adsorption and adsorbed phase heat capacity. The parameter values and ranges investigated are shown in Table 1. They correspond to values typically encountered in gas adsorption systems.

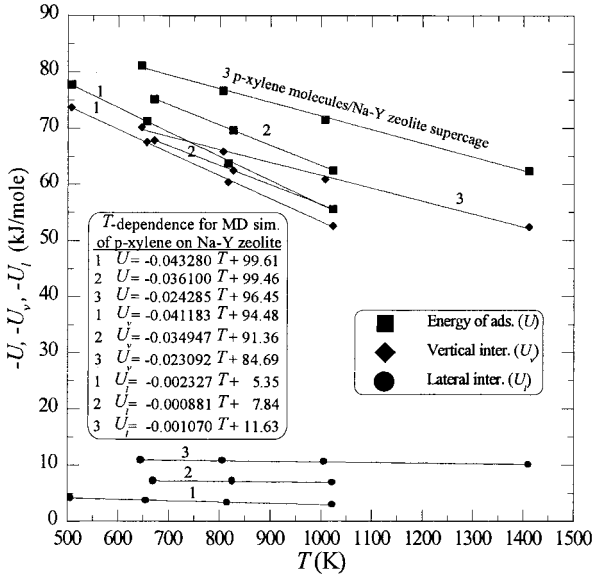

Figure 1. MD simulations for the adsorption of *p*-xylene on Na−Y zeolite.[8] The numbers on the fitted lines indicate the average number of *p*-xylene molecules per zeolite supercage used in the simulations.

Effect of Temperature (cases A, B, and C). Figures 2−4 show the effect of temperature on the isosteric heat of adsorption and adsorption equilibria at negligible, moderate, and relatively high surface heterogeneities, respectively. Each of these figures also shows the effect of favorable (negative), negligible, and unfavorable (positive) lateral interactions. The parameter values and ranges investigated for Figures 2, 3, and 4 are given in cases A, B, and C in Table 1, respectively. Figure 2 shows the combined effect of temperature and lateral interactions on a relatively homogeneous-adsorbent surface (i.e., with negligible heterogeneity). Clearly, for a homogeneous adsorbent, temperature has no effect on the isosteric heat of adsorption at all surface coverages. An examination of eq 7 with $s \rightarrow 0$ also reveals this fact. The isosteric heat of adsorption at zero-fractional-surface coverage is independent also of lateral interactions, as expected from eq 8. However, favorable (negative) lateral interactions on a homogeneous surface cause the isosteric heat of adsorption to increase with increasing surface coverage, as shown in Figure 2a. The results in Figure 1 potentially satisfy these conditions because the energy of adsorption increases with an increase in the number of *p*-xylene molecules per zeolite super cage, implying that attractive (favorable) interactions exist between the *p*-xylene molecules and that they are adsorbed on only a slightly heterogeneous adsorbent. However, when no lateral interactions exist on a homogeneous surface, as shown in Figure 2b, surface coverage has no effect on the isosteric heat of adsorption, as expected from this ideal situation and as revealed from eq 7 with s and $\omega \rightarrow 0$. In contrast, unfavorable

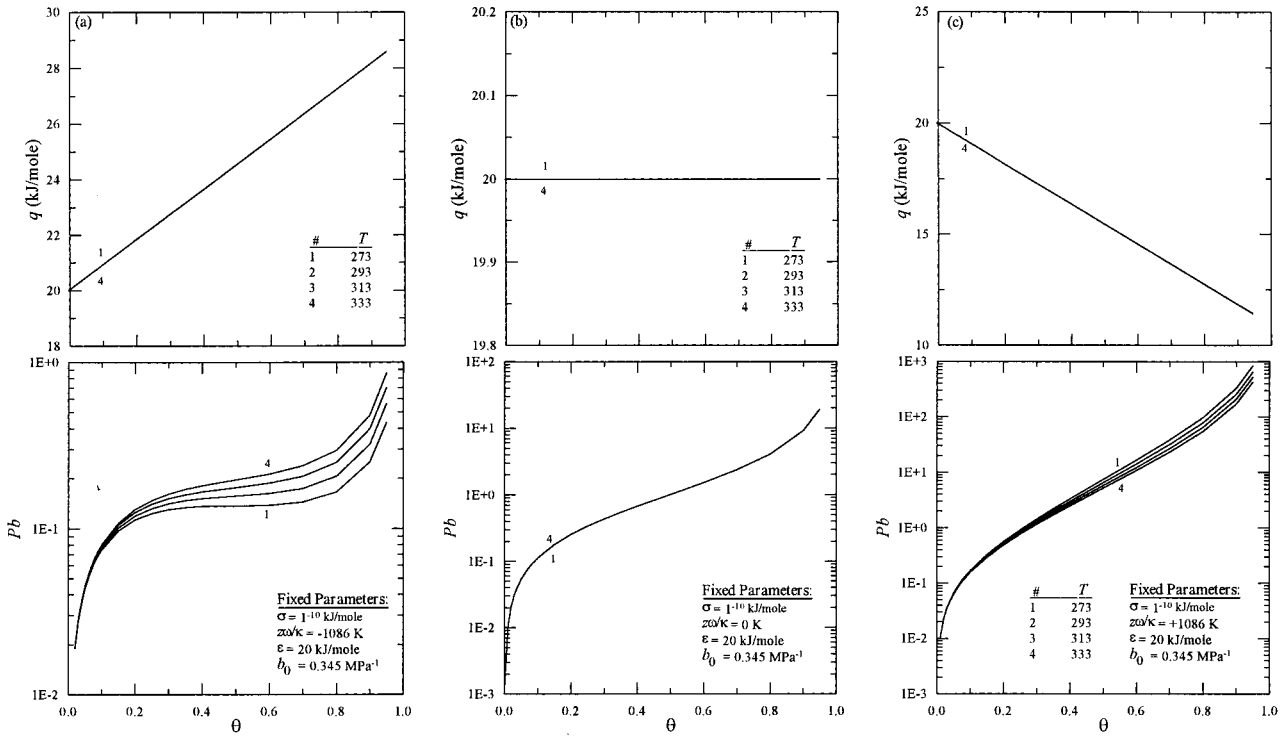

Figure 2. The effect of temperature on the isosteric heat of adsorption and adsorption equilibria with negligible surface heterogeneity and (a) favorable, (b) negligible, and (c) unfavorable lateral interactions.

(positive) lateral interactions decrease the isosteric heat of adsorption with increasing surface coverage, as shown in Figure 2c.

As an aside, it is interesting to point out that the adsorption isotherms are plotted in a characteristic form, i.e., Pb vs θ.[31] In this form, all of the isotherms should collapse into a single curve that is independent of temperature. This behavior is observed only in Figure 2b for noninteracting molecules adsorbed on a homogeneous adsorbent. In contrast, when lateral interactions are present, deviations from the ideal characteristic curve begin to appear at relatively high surface coverages where lateral interactions become appreciable. Parts a and c of Figure 2 show that when lateral interactions exist, systematic deviations from the characteristic curve occur, wherein Pb increases significantly with an increase in temperature at a fixed surface coverage for favorable interactions (Figure 2a) and decreases for unfavorable lateral interactions (Figure 2c). These deviations in Pb with temperature are interesting in that they disclose very clearly how departures from ideality manifest in the adsorption isotherm and they indicate an increasing sensitivity of the adsorption equilibria to variations in temperature when lateral interactions are encountered. These effects also produce a change in the amount adsorbed at a fixed Pb when compared to the ideal case presented in Figure 2b: favorable lateral interactions cause an increase, whereas unfavorable cause a decrease. These results are in agreement with the general concept of favorable and unfavorable lateral interactions and with previous analyses of the effects of these parameters on the adsorption equilibria.[4]

Figures 3 and 4 show the same conditions as those shown previously in Figure 2 but at higher degrees of adsorbent surface heterogeneity. Temperature effects on the isosteric heat of adsorption start to appear gradually in these two cases, which indicates that the temperature-dependence of the isosteric heat of adsorption is determined mainly by surface heterogeneity. The effect of temperature also becomes most pronounced at an intermediate level of surface heterogeneity, as noticed in Figure 3. However, temperature has only a minor effect on the isosteric heat of adsorption at all degrees of lateral interactions and surface coverages. Comparing the zero-surface-coverage isosteric heat of adsorption in Figures 2−4 shows that it increases significantly with increasing adsorbent surface heterogeneity and is independent of lateral interactions; these dependencies are evident from eq 8. Therefore, the temperature dependency and the zero-surface coverage of the isosteric heat of adsorption can be altered only by a heterogeneous surface. Surface heterogeneity also overcomes the effects of lateral interactions on the isosteric heat of adsorption; thus, the increase of the isosteric heat of adsorption with increasing surface coverage that is noticed in Figure 2a for favorable interactions on a homogeneous surface is no longer apparent in Figures 3a and 4a. Nevertheless, lateral interactions still play a role in the behavior of the isosteric heat of adsorption with surface coverage, but it is coupled with surface heterogeneity.

Figures 3 and 4 also show that in progressing from favorable to none to unfavorable lateral interactions, the gradient in the isosteric heat of adsorption with surface coverage increases dramatically. This gradient increases just as sharply with an increase in surface heterogeneity (compare Figure 3b with Figure 4b). Clearly, the effects of favorable lateral interactions, which are more physically realistic, oppose the effects of surface heterogeneity by causing less of a decrease in the isosteric heat of adsorption with increasing surface coverage compared to the ideal case with no lateral interactions.

Again, as an aside, it is interesting to note the behavior of the characteristic curve, i.e., Pb vs θ in Figures 3 and 4. Except for highly favorable lateral interactions on a moderately heterogeneous surface (Figure 3a), or favorable or unfavorable interactions on a homogeneous surface (parts a and c of Figure 2), deviations from the characteristic, temperature-independent behavior are observed in all cases at both low and high surface coverages, except for $Pb = 1$ where all of the curves in each case intersect and, thus, produce the characteristic behavior at

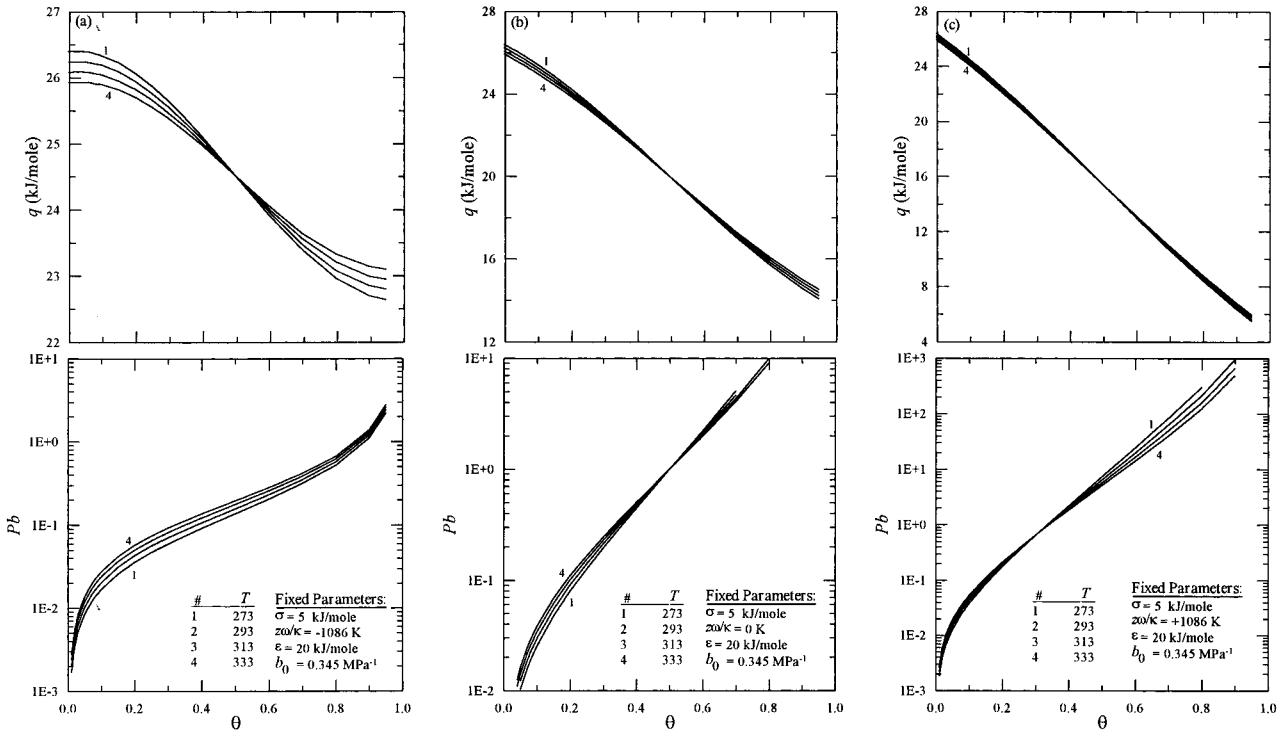

Figure 3. The effect of temperature on the isosteric heat of adsorption and adsorption equilibria with moderate surface heterogeneity and (a) favorable, (b) negligible, and (c) unfavorable lateral interactions.

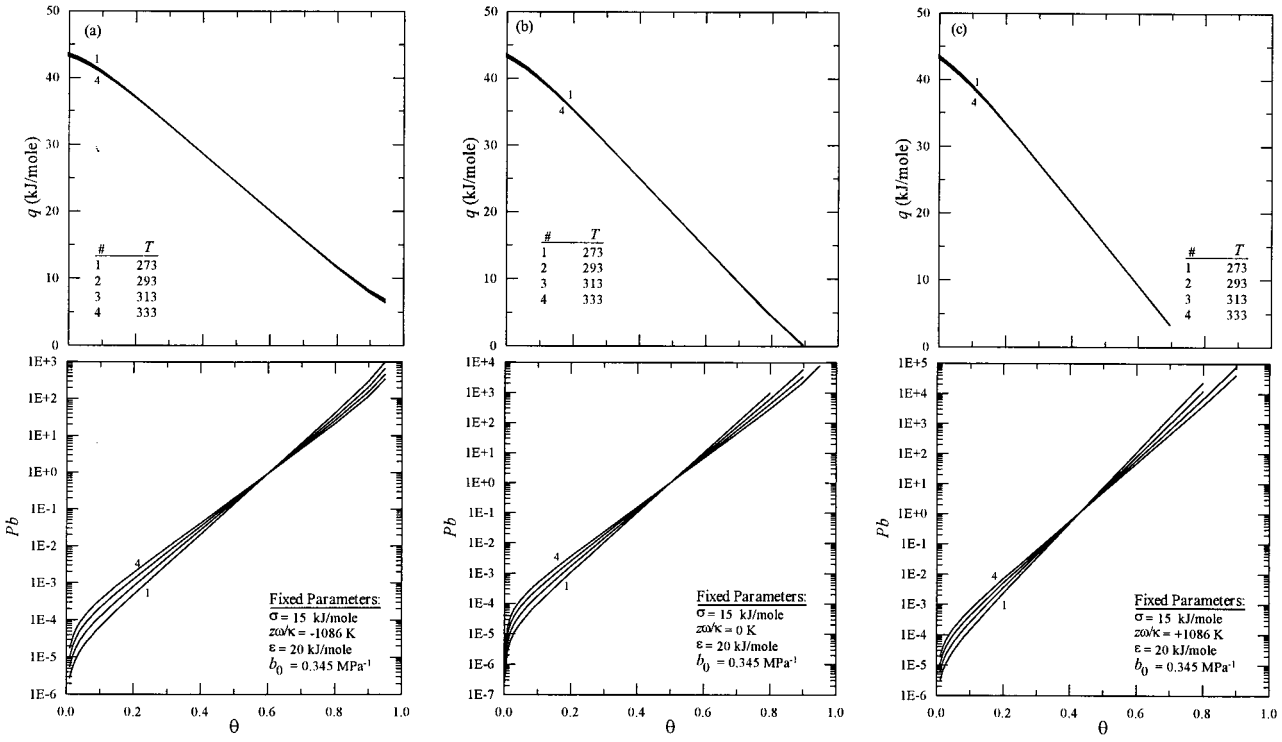

Figure 4. The effect of temperature on the isosteric heat of adsorption and adsorption equilibria with relatively high surface heterogeneity and (a) favorable, (b) negligible, and (c) unfavorable lateral interactions.

one point. This point of intersection switches the direction of the departure from the characteristic curve, similarly to the way lateral interactions do in Figure 2. It is also where the opposing effects of surface heterogeneity and lateral interactions exactly cancel producing ideal behavior. The variation of this point of intersection with surface coverage for different values of s and ω can be obtained by setting $Pb = 1$ in eq 1, which results in the following implicit (because of α) expression for θ:

$$\theta = \frac{1}{2s}\ln\left(\frac{1 + e^{s}e^{-\alpha}}{1 + e^{-s}e^{-\alpha}}\right) \tag{16}$$

Solving eq 16 iteratively for θ shows that when no lateral interactions dominate, this intersection point also corresponds to $\theta = 0.5$ but increases significantly or decreases slightly from this value when extremely favorable or unfavorable lateral

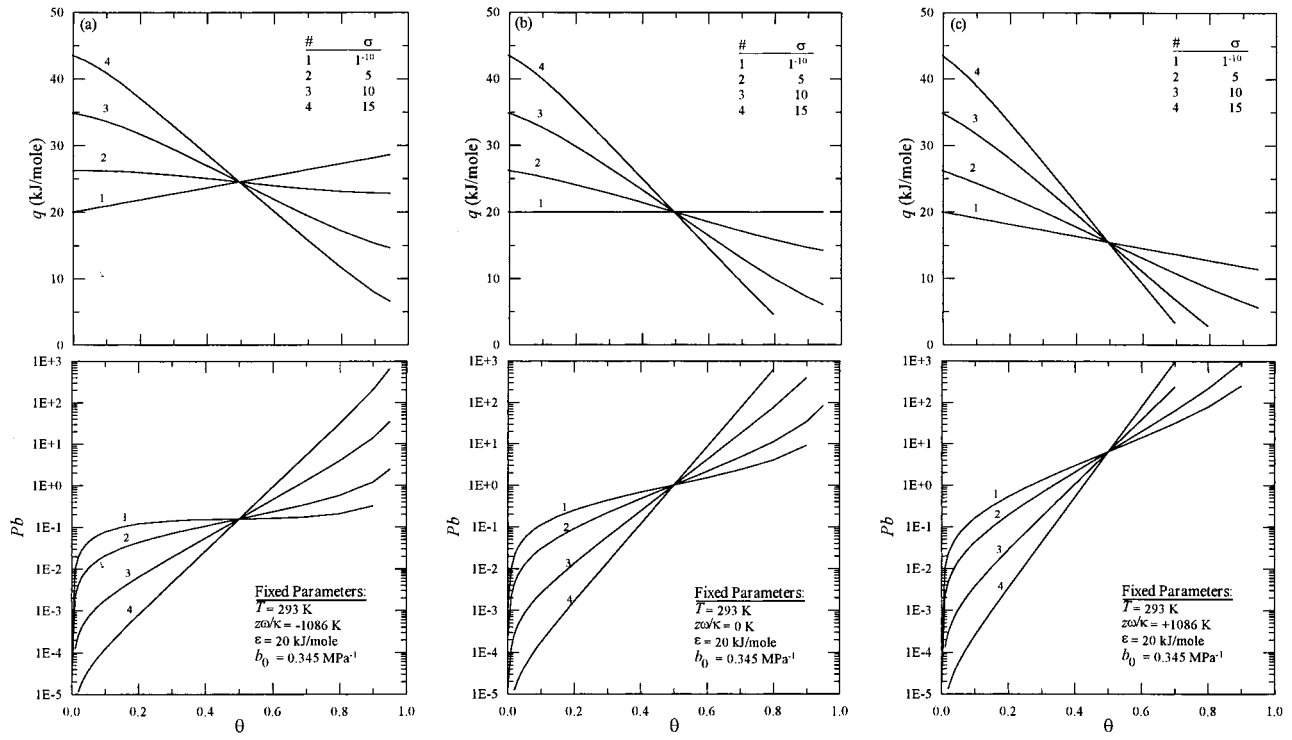

Figure 5. The effect of surface heterogeneity on the isosteric heat of adsorption and adsorption equilibria at moderate temperatures and (a) favorable, (b) negligible, and (c) unfavorable lateral interactions.

interactions exist, respectively. These strong dependencies are shown clearly in Figures 3 and 4.

Effect of Surface Heterogeneity (Case D). Figure 5 shows the effect of different degrees of surface heterogeneity on the isosteric heat of adsorption and adsorption equilibria at a moderate temperature (293 K) for (a) favorable, (b) negligible, and (c) unfavorable lateral interactions. The parameter values and ranges investigated are summarized in case D in Table 1. These curves show that when no lateral interactions exist (Figure 5b) and for a homogeneous surface (curve 1), the isosteric heat of adsorption is independent of surface coverage with a value equal to the adsorption energy, ϵ. As the heterogeneity of the surface increases, however, the isosteric heat of adsorption becomes an increasingly stronger and always decreasing function of surface coverage. Favorable lateral interactions on a homogeneous surface (Figure 5a, curve 1) cause the isosteric heat of adsorption to increase with increasing fractional-surface coverage. As the heterogeneity of the surface increases in this case, the effects of favorable lateral interactions are progressively overcome to the point where the isosteric heat of adsorption becomes independent of surface coverage, exhibiting the behavior of a homogeneous surface with no lateral interactions, and then it becomes an increasingly stronger and always decreasing function of surface coverage. In contrast to favorable lateral interactions, unfavorable lateral interactions cause the isosteric heat of adsorption to decrease with increasing surface coverage, even on a homogeneous surface (Figure 5c, curve 1). So in this case, unfavorable lateral interactions enhance the effects of surface heterogeneity and cause an even more pronounced but similar dependence of the isosteric heat of adsorption on the surface coverage as that shown in Figure 5b.

Figure 5 also shows that the variation of the zero-surface-coverage isosteric heat of adsorption with surface heterogeneity is much higher than that with temperature, which is shown in Figures 3 and 4. These results imply that the effects of surface heterogeneity are more pronounced than those of lateral interactions and noticeably more important than temperature in determining the behavior of the isosteric heat of adsorption. These results also agree with the more rigorous but less insightful MD simulations[8] shown in Figure 1, in terms of the relative contributions of lateral and vertical interactions as well as the relative contribution of temperature to the energy of adsorption.

The adsorption equilibria also show some interesting behavior that is indicative of the mathematical symmetry of this simple lattice model; i.e., all of the curves intersect at $\theta = 0.5$. The mathematical implications of this behavior have been discussed in detail by Hill[10,32] and also by Rudzinski and Everett;[33] therefore, only the physical implications are discussed herein. It is noteworthy that the similar behavior noted in a previous section, where most of the curves cross at $Pb = 1.0$ (see the adsorption equilibria in Figures 3 and 4) instead of $\theta = 0.5$, has not been discussed in the literature. Nevertheless, the behavior shown in Figure 5 indicates that the effects of heterogeneity cancel out at this point of intersection. It also shows that the reduced pressure and isosteric heat of adsorption corresponding to this point of intersection, denoted as bP^* and q^*, are functions of the lateral interaction parameter.[4] Substituting $\theta = 0.5$ in eqs 5 and 7 gives these functionalities as

$$bP^*_{\theta=0.5} = \exp\left(\frac{z\omega}{2\kappa T}\right) \tag{17}$$

$$q^*_{\theta=0.5} = \epsilon - \frac{R}{2}\left(\frac{z\omega}{\kappa}\right) \tag{18}$$

These relations show, for example, that when no lateral interactions exist, all of the adsorption equilibria curves cross at $bP^* = 1.0$, and all of the isosteric heat of adsorption curves cross at $q^* = \epsilon$, i.e., the average adsorption energy (20 kJ/mol), regardless of surface heterogeneity.

This mathematical symmetry also has some interesting implications with respect to the characteristic curve (Pb vs θ).

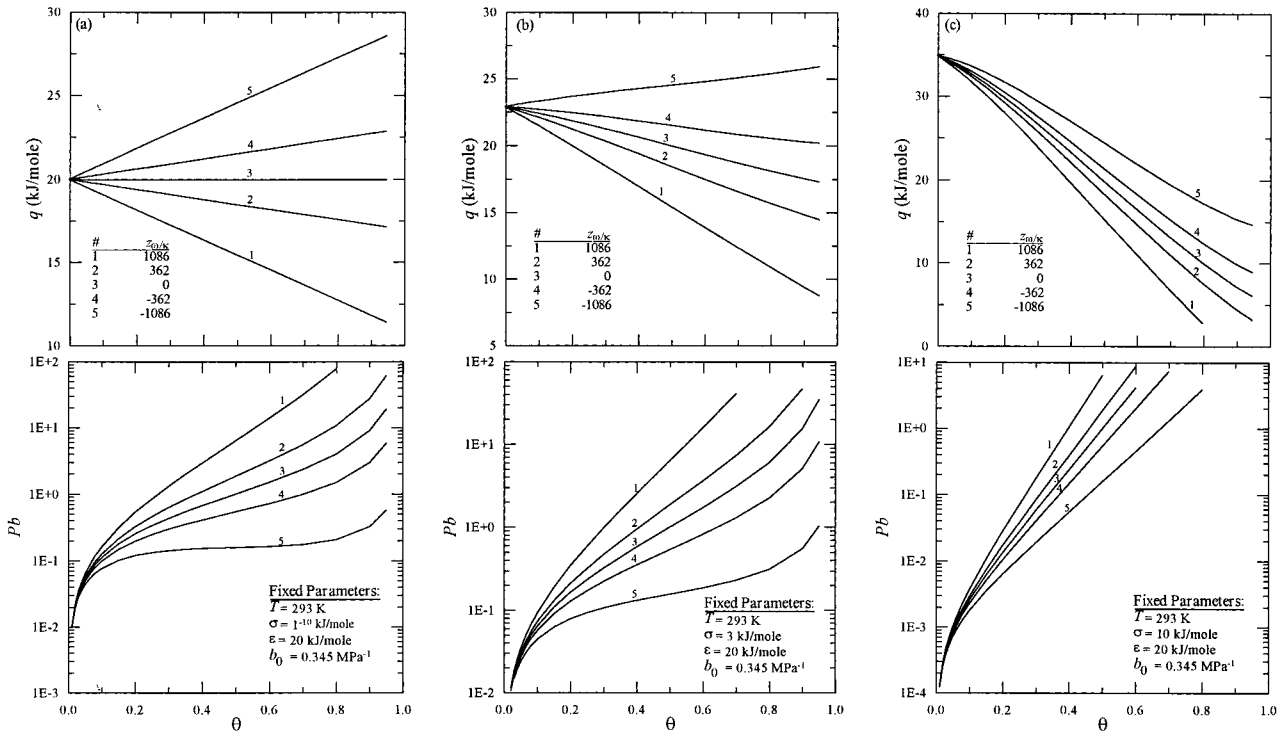

Figure 6. The effect of lateral interactions on the isosteric heat of adsorption and adsorption equilibria at moderate temperatures and (a) negligible, (b) moderate, and (c) relatively high surface heterogeneities.

The ideal situation is curve 1 in Figure 5b, where s and $\omega \rightarrow 0$ and $q = \epsilon$ and is independent of surface coverage. All of the other curves deviate significantly from this ideal behavior, except for curves 1−4 in Figure 5b but only at the point of intersection. Nevertheless, in all cases, as heterogeneity increases the departure from ideality switches from negative deviations for surface coverages less than $\theta = 0.5$ to positive deviations for those greater than $\theta = 0.5$. Negative deviations from ideality are defined herein as those corresponding to a higher loading for a given Pb. The effect of favorable lateral interactions enhances this behavior by shifting all of the curves to lower values of Pb, as shown in Figure 5a where the point of intersection at $\theta = 0.5$ is shifted from $Pb = 1.0$ in the ideal case to $Pb \cong 0.1$. The opposite behavior is caused by unfavorable lateral interactions. These results show very clearly the coupled and marked effects of lateral interactions and surface heterogeneity on the departure from ideality.

Effect of Lateral Interactions (Case E). Figure 6 shows the effect of lateral interactions on the isosteric heats of adsorption and adsorption equilibria at a moderate temperature (293 K) for (a) relatively homogeneous, (b) moderately heterogeneous, and (c) highly heterogeneous surfaces. The parameter values and ranges investigated are summarized in case E in Table 1. The fact that adsorbate−adsorbate lateral interactions have no effect on the zero-surface-coverage isosteric heat of adsorption is very clearly exhibited in Figure 6, where all of the curves intersect at the same value of the isosteric heat of adsorption at zero-surface coverage; however, this value increases with increasing surface heterogeneity, as depicted in eq 8. It is noteworthy to recognize that although the second term in eq 8 appears to be an increasing linear function of temperature (because of RT), it normally exhibits decreasing trends, as shown in Figures 3 and 4. The reason is due to the opposite temperature dependence of s which, when included in the exponential form of eq 8, overcomes the effect of RT. Therefore, as noticed previously for the isosteric heat of adsorption at all surface coverages, the temperature dependence of the zero-coverage isosteric heat of adsorption is related closely to the magnitude of surface heterogeneity.

For both the homogeneous (Figure 6a) and slightly heterogeneous (Figure 6b) surfaces, essentially the same trends are observed, where the isosteric heat of adsorption progresses from a decreasing linear function of the surface coverage to an increasing linear function as the lateral interactions change from unfavorable to favorable. However, for a very heterogeneous surface, the isosteric heat of adsorption always decreases with increasing surface coverage, but less so as the lateral interactions change from unfavorable to favorable. The functions also become slightly nonlinear exhibiting some sigmoidal character. These results show very clearly the complex interplay between lateral interactions and heterogeneity, both of which have a marked effect on the way the isosteric heat of adsorption varies with surface coverage.

The characteristic curve (Pb vs θ) also deviates significantly from the ideal behavior except at very low surface coverages. The ideal curve is actually curve 3 in Figure 6a, which is clearly noted by the isosteric heat of adsorption being independent of surface coverage. Moreover, in progressing from unfavorable to none to favorable lateral interactions, the trends are the same for both homogeneous and heterogeneous surfaces, where all of the departures from ideality progress from positive deviations to negative deviations, where negative deviations correspond to a higher loading for a given Pb, as defined previously.

Effects of Surface Heterogeneity, Fractional Surface Coverage, Lateral Interactions, and Temperature on the Adsorbed Phase Heat Capacity. Figures 7 and 8 show the effects of the fractional coverage, adsorbent heterogeneity, and temperature on the difference between the differential adsorbed and molar gas phase heat capacities, and Figure 9 shows the same effects, along with lateral interactions, on the difference between the molar adsorbed and molar gas phase heat capacities. As the temperature dependence of the isosteric heat of adsorption on a homogeneous surface is always negligible (see Figure 2), the surface heterogeneity is varied from slight to relatively high

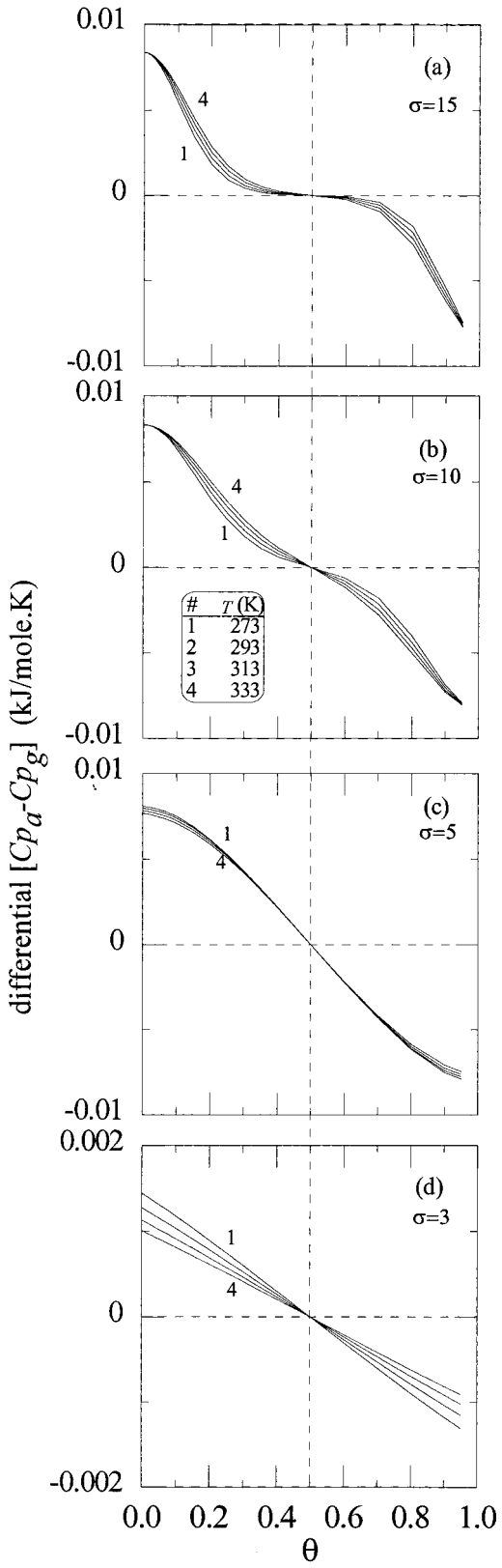

Figure 7. The difference between the differential adsorbed and molar gas phase heat capacities for different surface heterogeneities and temperatures.

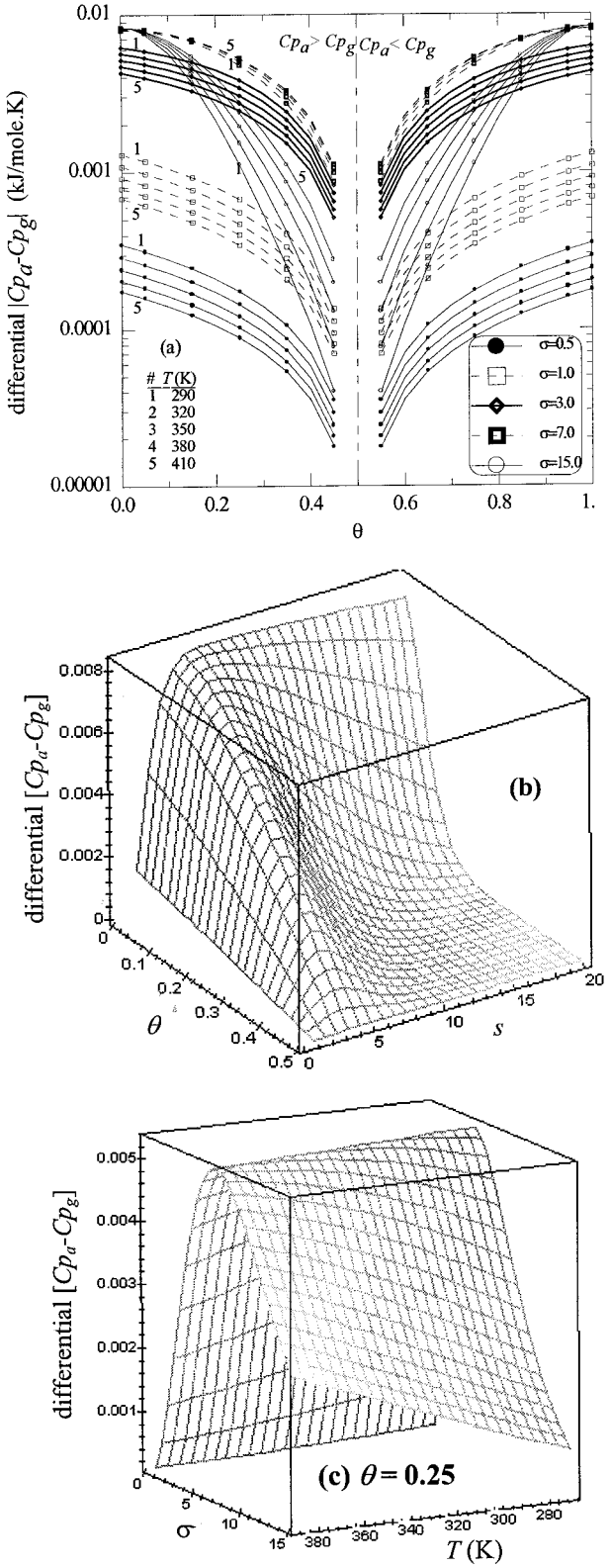

Figure 8. Detailed temperature and heterogeneity dependence of the differential adsorbed phase heat capacity (a) over the entire range of fractional surface coverage, (b) at a focused view over $0 \lesssim \theta \lesssim 0.5$, and (c) for a profile at a fractional surface coverage of 0.25.

values. The parameter values and ranges investigated are summarized in case F in Table 1. Recall from eq 12 that, according to this model, lateral interactions have no effect on the differential adsorbed phase heat capacity and that this result is in agreement with the MD simulations in the literature.[8] The results in Figures 7 and 8 show that the effect of temperature on the adsorbed phase heat capacity is also minimal, but the effects of fractional surface coverage and adsorbent heterogeneity are relatively more pronounced.

Figure 7 shows the overall trends for the difference between the differential adsorbed and molar gas phase heat capacities ($\Delta\bar{C}_{p_a}$) for moderately to highly heterogeneous surfaces. In all

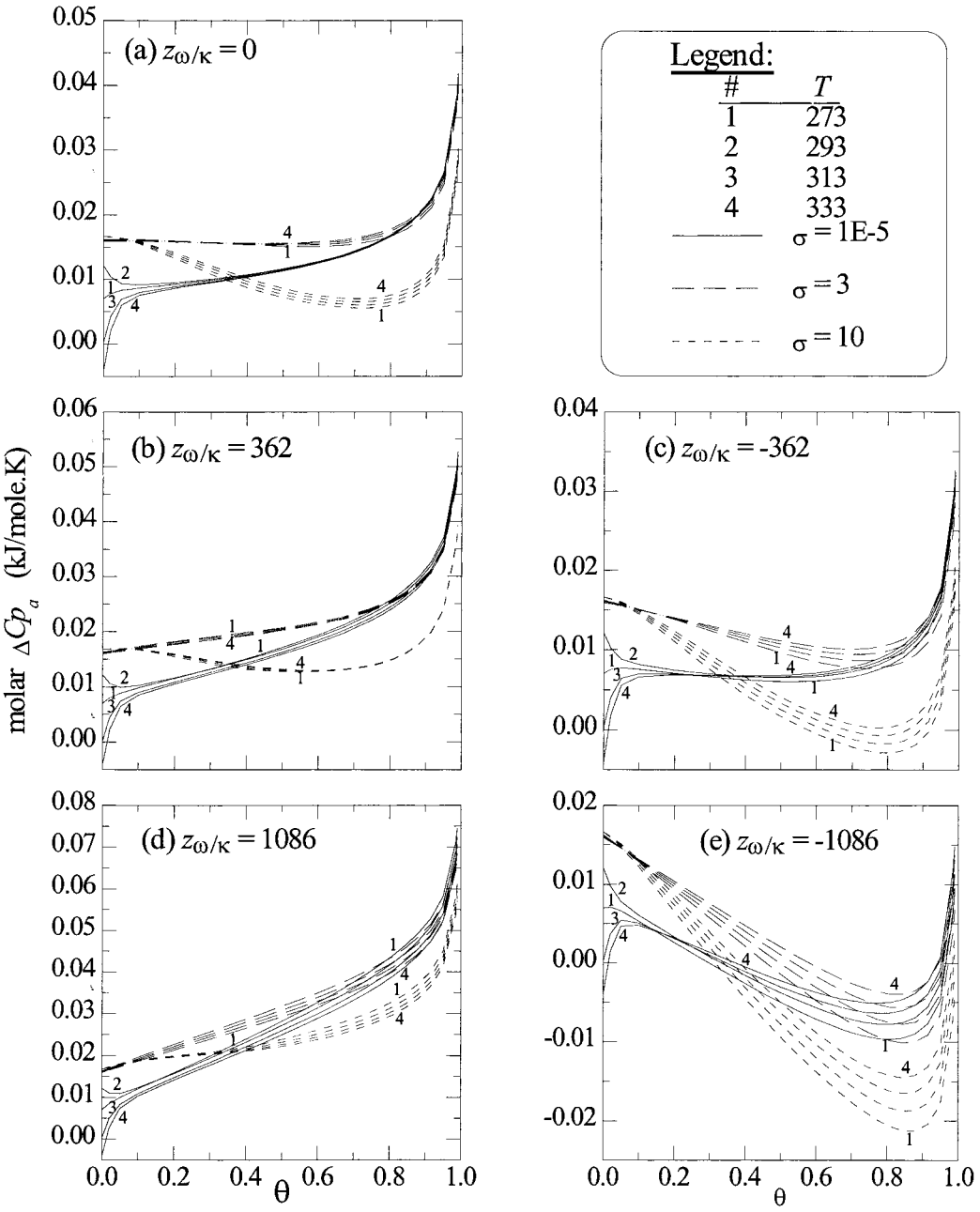

Figure 9. Effects of surface coverage, surface heterogeneity, lateral interactions, and temperature on the difference between the molar adsorbed and gas-phase heat capacities.

cases, this difference is a decreasing function of surface coverage, exhibiting nearly linear behavior for the moderately heterogeneous surface to highly sigmoidal behavior for the highly heterogeneous surface. Moreover, the differential adsorbed phase heat capacity is higher than the molar gas phase heat capacity at loadings below $\theta = 0.5$, lower than the gas phase heat capacity at loadings above $\theta = 0.5$, and equal to zero at $\theta = 0.5$, with marked deviations from zero on either side of $\theta = 0.5$. The breadth of the zero$-\Delta\bar{C}_{p_a}$ region around $\theta = 0.5$ also increases considerably with increasing surface heterogeneity. The zero$-\Delta\bar{C}_{p_a}$ behavior at and around $\theta = 0.5$ is associated with the behavior of a homogeneous surface, where the effects of heterogeneity on the adsorption equilibria all coincide and, thus, cancel out, as shown in Figure 5. This behavior is consistent with a rigorous classical thermodynamic analysis[5,34] that shows the gas and adsorbed phase heat capacities to be equal for a homogeneous surface. Figure 7a−c also shows that regardless of whether the surface is moderately or highly heterogeneous, almost the same absolute values of $\Delta\bar{C}_{p_a}$ result at zero and full (100%) surface coverages; however, $\Delta\bar{C}_{p_a}$ is very small and decreases rapidly approaching nearly zero on slightly heterogeneous surfaces even at these two extremes in surface coverage, as shown in Figure 7d.

Figure 8a shows that $|\Delta\bar{C}_{p_a}|$ is essentially a mirror reflection around $\theta = 0.5$ but with opposite signs as shown in Figure 7. Figure 8 also shows that although this difference is very small at very low surface heterogeneities, it increases rapidly up to an optimum value at $\sigma_{opt} \approx 7$ and the corresponding temperatures. After this optimum, it becomes almost constant at zero- and full-surface coverages while gradually increasing the zero$-\Delta\bar{C}_{p_a}$ region around $\theta = 0.5$, as also noticed in Figure 7a−c. Figure 8b shows a focused view of this behavior for θ values less than 0.5. It also shows that the effect of surface heterogeneity at $\theta = 0$ is quite different than that at other loadings. At $\theta = 0$, $\Delta\bar{C}_{p_a}$ exhibits a maximum value at $s_{opt} = 1$, with the temperature contribution according to eq 2, and decreases very

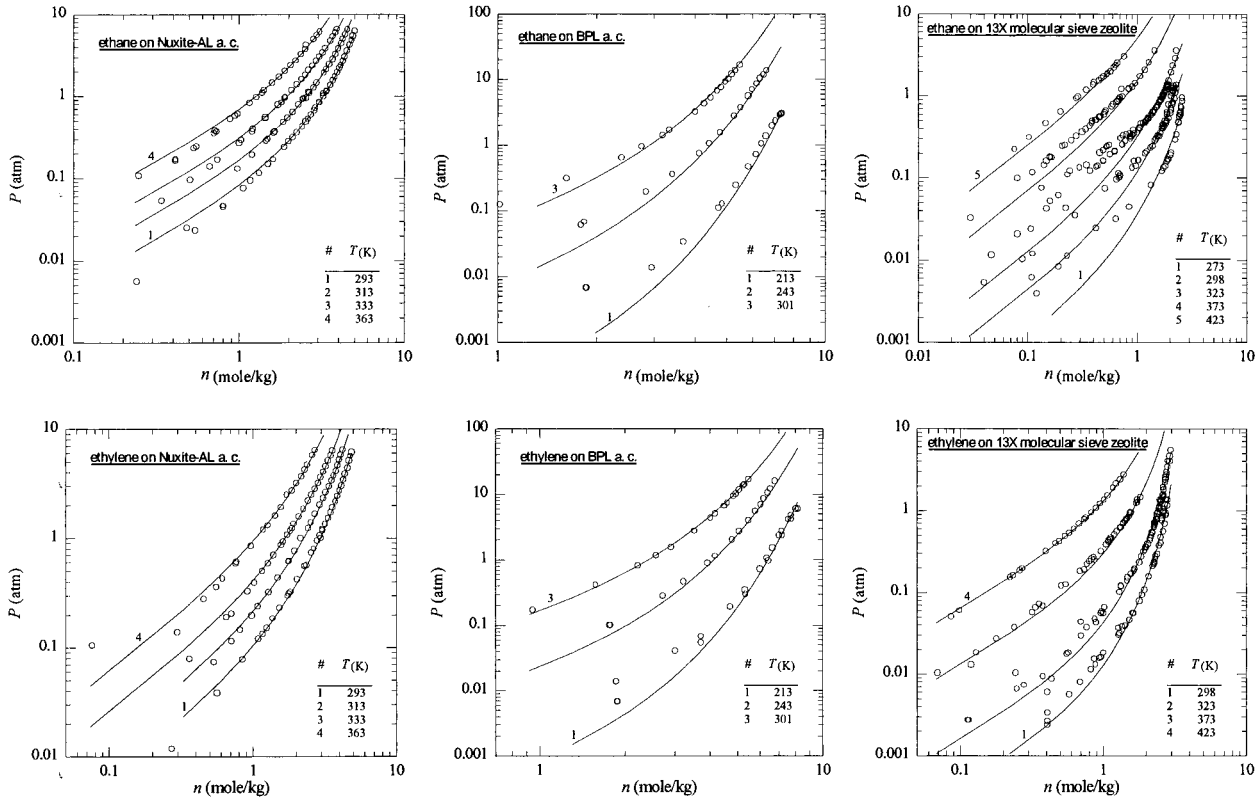

Figure 10. Single-component adsorption equilibria for ethane and ethylene on Nuxite−AL activated carbon,[35−36] BPL activated carbon,[37] and 13X molecular sieve zeolite.[38−40] Symbols and lines represent experimental and correlated data, respectively.

slowly with increasing surface heterogeneity. Such a decrease in $\Delta\bar{C}_{p_a}$ at zero-surface coverage and high-surface heterogeneity is not very apparent within moderate ranges of surface heterogeneity and is assumed negligible. At higher loadings, however, $\Delta\bar{C}_{p_a}$ also has a maximum value at an intermediate surface heterogeneity, after which it decreases more sharply with increasing surface coverage. Clearly, this intermediate *s* and the corresponding $\Delta\bar{C}_{p_a}$ values decrease as $\theta \rightarrow 0.5$, causing the zero−$\Delta\bar{C}_{p_a}$ effect around $\theta = 0.5$, which is also noticed before in Figure 7. Figure 8c shows this behavior, as well as the effect of temperature, at the middle of the low surface coverage region, i.e., at $\theta = 0.25$. The contour lines in Figure 8c show that the temperature dependence of the differential adsorbed phase heat capacity inverts at the optimum surface heterogeneity, σ_{opt}. These contours also show that $\Delta\bar{C}_{p_a}$ decreases more slowly with increasing temperature at low surface heterogeneities compared to that at high surface heterogeneities. However, the temperature dependence in both cases is negligibly weak relative to the effect of surface heterogeneity, especially at moderate surface heterogeneities.

Figure 9 shows the difference between the molar adsorbed and gas phase heat capacities after trapezoidal integration of the results from the loading dependence of eqs 5, 7, and 12, according to eq 15, and over very small increments of fractional-surface coverage. Overall, the strongest factor affecting the difference between the molar adsorbed and gas phase heat capacities is the surface coverage. Zero-surface coverage behavior is completely independent of the lateral interactions, whereas the difference between the molar adsorbed and gas phase heat capacities increases dramatically when $\theta \rightarrow 1$. Lateral interactions show a more pronounced effect at relatively high surface coverages, wherein the adsorbed phase heat capacity increases when the lateral interactions change from negative (attractive) to positive (repulsive). An optimum temperature dependence is always exhibited on homogeneous surfaces at low surface coverages resulting in higher adsorbed phase heat capacities at moderate temperatures. Also, as noticed in the differential adsorbed phase heat capacity, $\Delta\tilde{C}_{p_a}$ at low surface coverages and moderate to high surface heterogeneities is almost constant. However, highly heterogeneous surfaces exhibit a sharper decrease in $\Delta\tilde{C}_{p_a}$ when increasing the surface coverage until reaching a minimum value at a surface coverage of ~0.8. This decrease becomes more pronounced when highly negative lateral interactions are exhibited. Nevertheless, $\Delta\tilde{C}_{p_a}$ always approaches infinity when $\theta \rightarrow 1$, regardless of any other conditions. $\Delta\tilde{C}_{p_a}$ can be negative (resulting in a molar adsorbed phase heat capacity that is less than the gas phase heat capacity) only when highly negative lateral interactions are exhibited or at very low surface coverages and high temperatures.

Correlation with Literature Data. The applicability of this model to predict the isosteric heat of adsorption and adsorbed phase heat capacity from eqs 7 and 12 or 14, respectively, based on single-component adsorption-isotherm data correlated with eq 5 is examined using experimental data from the literature.[35−40] Figures 10 and 11, respectively, display the correlated adsorption equilibria and predicted isosteric heats of adsorption and adsorbed phase heat capacities for ethane and ethylene adsorbed by Nuxite−Al activated carbon,[35−36] BPL activated carbon,[37] and 13X molecular sieve zeolite.[38−40] Figure 10 shows that eq 5 satisfactorily correlates single-component adsorption equilibria over relatively wide ranges of temperature and with reasonable errors. The fitted parameters and absolute relative errors (ARE) in the equilibrium pressure of each system are given in Table 2. This satisfactory performance certainly adds more reliability to the predicted thermodynamic properties shown in Figure 11, i.e., the isosteric heats of adsorption and the percent deviation between the molar adsorbed and gas phase heat capacities. Moreover, Figure 11 shows that the predicted values of the

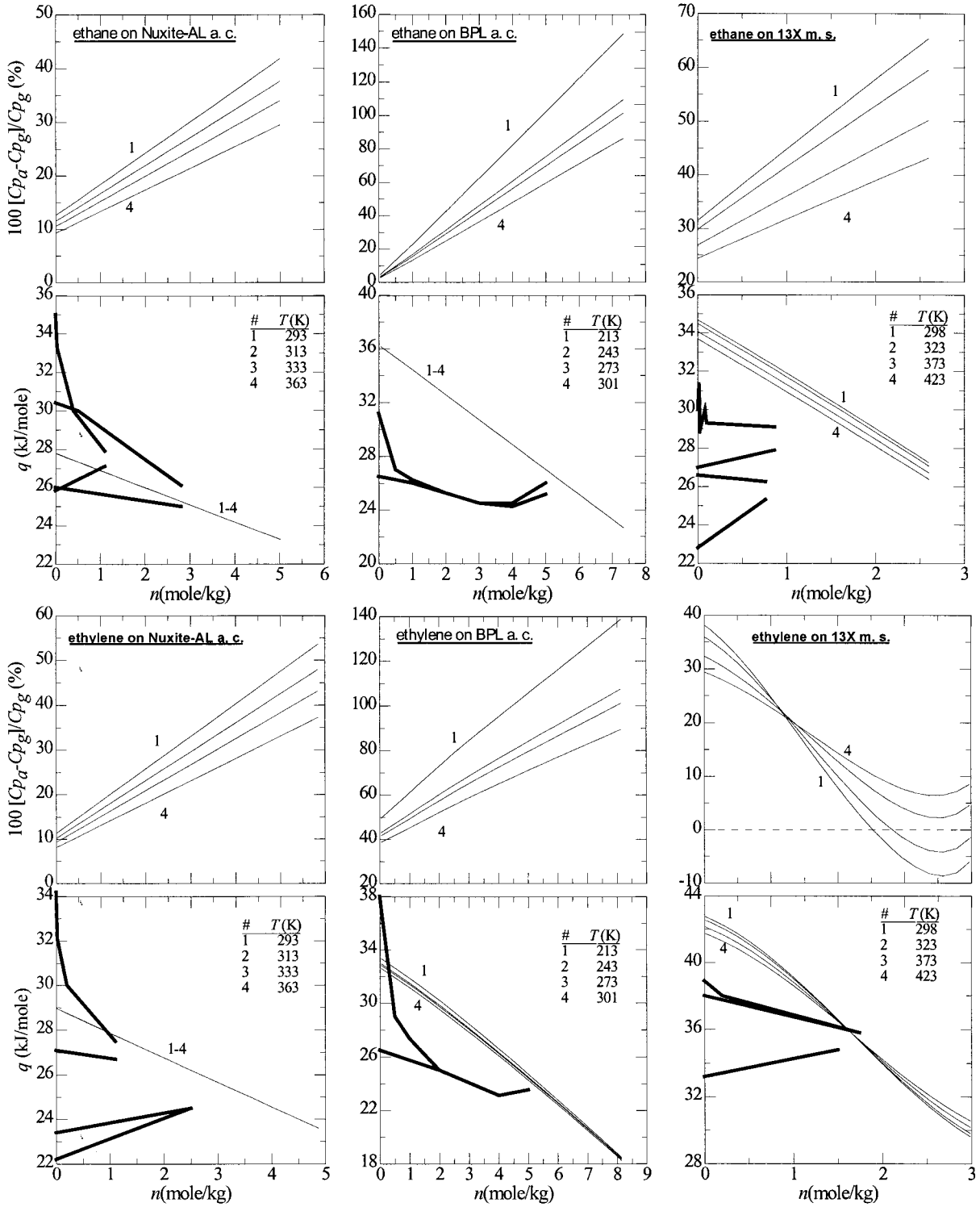

Figure 11. Predicted isosteric heats of adsorption and percent deviations of the molar adsorbed phase heat capacity from the molar gas phase heat capacity for ethane and ethylene on Nuxite−AL activated carbon.[35−36] BPL activated carbon[37] and 13X molecular sieve zeolite.[38−40] Thick lines indicate temperature-independent estimations from the literature[25] using Toth and UNILAN isotherm models.

isosteric heats of adsorption in most cases agree well with those reported in the literature using the UNILAN and Toth models and the chain rule version of the Clausius−Clapeyron equation.[25] Some cases, however, showed remarkable differences between the values predicted in this work and the literature values as well as between the literature values themselves when calculated with different models. In all cases, both the isosteric heat of adsorption and relative differences between the adsorbed and gas phase molar heat capacities decrease with an increase in the amount adsorbed, the former result being indicative of a heterogeneous adsorbent. A more important and more interesting result, however, is the very subtle effects of the temperature dependence of the isosteric heat of adsorption on the difference between the adsorbed and gas phase molar heat capacities.

When there is no observable temperature dependence of the isosteric heat of adsorption, negligible differences result between the adsorbed and gas phase molar heat capacities, in agreement with the classical thermodynamic analysis carried out by Sircar.[5,34] This is the case for ethane and ethylene on Nuxite−Al activated carbon and for ethane on BPL activated carbon.

TABLE 2: Regression Parameters and ARE[a] Values for the Adsorption Isotherms of Ethane and Ethylene on Different Adsorbents Fitted to Eq 5 Using the Least-Sum-Square-Error in Equilibrium Pressures

adsorbent	adsorbate	b_0 (10^{-6} atm^{-1})	ϵ/R (K)	$z\omega/\kappa$ (K)	σ/R (K)	m (mol/kg)	*ARE* (%)[a]
Nuxite−AL activated carbon[35−36]	ethane	33.854	3337	727	36.720	6.723	8.49
	ethylene	13.674	3482.	1140	24.480	8.628	5.99
BPL activated carbon[37]	ethane	1.440	4365	2666	3.421	11.935	21.66
	ethylene	3.675	1705	4694	1460.007	39.678	13.99
13X molecular sieve zeolite[38−40]	ethane	3.908	3143	4692	765.715	18.261	23.72
	ethylene	8.959	3994	−611	835.573	3.312	14.05

[a] $\text{ARE} = \frac{100\%}{N}\sum_{i=1}^{N}\frac{|P_i^{\text{corr}} - P_i^{\text{exp}}|}{P_i^{\text{exp}}}$; N = total number of experimental data points.

However, a very slightly temperature-dependent isosteric heat of adsorption leads to appreciable differences between the adsorbed and gas phase molar heat capacities with relative increases above the gas phase molar heat capacity ranging between 11 and 24%. This is the case for ethylene on BPL activated carbon and ethane and ethylene on 13X molecular sieve zeolite. This temperature dependence of the isosteric heat of adsorption, and therefore the difference between the adsorbed and gas phase heat capacities, arises from the optimized value of the surface heterogeneity term (i.e., σ); thus, without experimental verification, these results are somewhat speculative. Nevertheless, their implications to the design and modeling of adsorption processes cannot be overlooked.

Despite the almost weak temperature dependence of the isosteric heat of adsorption and the mostly negligible deviations between the adsorbed and gas phase molar heat capacities, such temperature dependencies and heat capacity deviations can be extremely important, especially when these heat capacity deviations can reach values on the order of +20%. These deviations also increase at lower temperatures, but the effect of temperature on the adsorbed phase heat capacity is shown to be less important than those of surface heterogeneity and fractional surface coverage in the parametric study (see Figures 7−9). Moreover, these results agree with those in the parametric study which show similar deviations between the heat capacities, with predicted differences on the order of 10^{-2} kJ/(mol K) as shown in Figures 7−9. Considering that the gas phase molar heat capacities of components typically separated in industrial adsorption processes are on the order of 0.05−0.15 kJ/(mol K), adding such corrections to the gas phase heat capacities can have a remarkable effect on the simulation of such processes. This is especially true if the simulations are performed at conditions where temperature effects on both the thermodynamic properties and the process itself become important, like those shown recently by Liu and Ritter in the simulation of a pressure swing adsorption process.[41]

Conclusions

New analytic expressions for the isosteric heat of adsorption and differential adsorbed phase heat capacity are derived from an extension of the Fowler−Guggenheim adsorption isotherm to account for a random heterogeneous surface based on a uniform distribution of energies. The new expressions provide a satisfactory and consistent description of the isosteric heat of adsorption and the adsorbed phase heat capacity in terms of fractional surface coverage, temperature, heterogeneity, and lateral interactions. A parametric study gives considerable insight into the roles of these parameters and shows that adsorbent surface heterogeneity, fractional surface coverage, and lateral interactions all have significant effects on the isosteric heat of adsorption. The zero-surface coverage isosteric heat of adsorption increases with increasing surface heterogeneity and is not affected by lateral interactions. Favorable (attractive) lateral interactions increase the isosteric heat of adsorption with increasing surface coverage on a homogeneous adsorbent; however, this effect is overcome easily when increasing the surface heterogeneity. The relative temperature dependence of the isosteric heat of adsorption depends mainly on the adsorbent surface heterogeneity and the fractional surface coverage; it also becomes most pronounced on surfaces with an intermediate heterogeneity of $s \approx 1$ and at zero or full (100%) fractional surface coverages. A homogeneous surface results in a temperature-independent isosteric heat of adsorption.

This study also shows that the differential adsorbed phase heat capacity depends on fractional surface coverage, surface heterogeneity, and temperature but not on lateral interactions. The differential adsorbed phase heat capacity is equal approximately to the gas phase molar heat capacity either at a fractional surface coverage of 0.5 or on a homogeneous surface. However, the molar adsorbed phase heat capacity is, in most cases, higher than that of the gas phase heat capacity and decreases with either decreasing surface heterogeneity or increasing fractional surface coverage. The deviations between the molar adsorbed and gas phase heat capacities is always important, especially at very high surface coverages, intermediate surface heterogeneities, or high lateral interactions (both repulsive and attractive). The effect of temperature on the adsorbed phase heat capacity is noticeable but less important than the effects of fractional surface coverage and adsorbent heterogeneity.

The applicability of this model to predict the isosteric heat of adsorption and the molar adsorbed phase heat capacity from experimental adsorption isotherm data is demonstrated also and shows satisfactory agreement with published results. Moreover, some of the systems examined exhibit a deviation between the molar adsorbed and gas phase heat capacities of ~20% above the gas phase molar heat capacity. Such a deviation results from the optimized heterogeneity parameter when it meets or approaches the optimum temperature dependence conditions, as illustrated in the parametric study. The magnitude of this deviation also has important implications in the modeling of adsorption processes that exhibit marked temperature effects.

Acknowledgment. The authors gratefully acknowledge financial support from the National Science Foundation, Westvaco Charleston Research Center, and Separations Research Program at the University of Texas at Austin.

References and Notes

(1) Barrer, R. M.; Coughlan, B. In *Molecular Sieves*; Society of Chemical Industry: London, 1968; pp 233−241.

(2) Maslan, F.; Abereth, E. R. *J. Chem. Eng. Data* **1972**, *17*, 286.
(3) Reich, R.; Ziegler, W. T.; Rogers, K. A. *Ind. Eng. Chem. Process Des. Dev.* **1980**, *19*, 336.
(4) Ritter, J. A.; Kapoor, A.; Yang, R. T. *J. Phys. Chem.* **1990**, *94*, 6785.
(5) Sircar, S. *Ind. Eng. Chem. Res.* **1991**, *30*, 1032.
(6) Al-Muhtaseb, S. A.; Ritter, J. A. *Ind. Eng. Chem. Res.* **1998**, *37*, 684.
(7) Al-Muhtaseb, S. A.; Ritter, J. A. *Langmuir* **1998**, *14*, 5317.
(8) Schrimpf, G.; Tavitian, B.; Espinat, D. *J. Phys. Chem.* **1995**, *99*, 10932.
(9) Battaglia, F.; Kim, Y. S.; George, T. F. *J. Phys. Chem.* **1987**, *91*, 414.
(10) Hill, T. L. *J. Chem. Phys.* **1949**, *17*, 762.
(11) O'Brien, J. A.; Myers, A. L. In *Fundamentals of Adsorption*; Myers, A. L, Belfort, G., Eds.; Engineering Foundation: New York, 1984.
(12) Russell, B.; LeVan, M. *Chem. Eng. Sci.* **1996**, *51*, 4025.
(13) Kaminski, R.; Monson, P. *AIChE J.* **1992**, *38*, 1979.
(14) Kaminski, R.; Monson, P. *Langmuir* **1993**, *9*, 561.
(15) Steele, W. *J. Phys. Chem.* **1964**, *67*, 2016.
(16) Jaroniec, M.; Patrykiejew, A. *Phys. Lett.* **1978**, *67A*, 309.
(17) Rudzinski, W.; Jagiello, J.; Grillet, Y. *J. Colloid Interface Sci.* **1982**, *87*, 478.
(18) Sircar, S.; Myers, A. L. *AIChE Symp. Ser.* **1984**, *80*, 55.
(19) Rudzinski, W.; Jagiello, J. *Adsorpt. Sci. Technol.* **1989**, *6*, 35.
(20) Karavias, K.; Myers, A. *Chem. Eng. Sci.* **1992**, *47*, 1441.
(21) Jagiello, J.; Schwarz, J. *Langmuir*. **1993**, *9*, 2513.
(22) Bakaev, V.; Steele, W. *Langmuir* **1996**, *12*, 6119.
(23) Gusev, V.; O'Brien, J. A.; Jensen, C. R.; Seaton, N. A. *AIChE J.* **1996**, *42*, 2773.
(24) Mathias, P. M.; Kumar, R.; Moyer, Jr., J. D.; Schork, J. M.; Srinivasan, S. R.; Auvil, S. R.; Talu, O. *Ind. Eng. Chem. Res.* **1996**, *35*, 2477.
(25) Valenzuela, D. P.; Myers, A. L. In *Adsorption Equilibrium Data Handbook*; Prentice Hall: Englewood Cliffs, NJ, 1989.
(26) Sircar, S. *Langmuir* **1991**, *7*, 3065.
(27) Sircar, S. *Ind. Eng. Chem. Res.* **1992**, *31*, 1813.
(28) Pan, H.; Ritter, J. A.; Balbuena, P. B. *Langmuir* **1998**, *14*, 6323.
(29) Hacskaylo, J. J.; LeVan M. D. *Langmuir* **1985**, *1*, 97.
(30) Ross, S.; Olivier, J. P. In *On Physical Adsorption*; Interscience: London, 1964.
(31) Ruthven, D. M. In *Principles of Adsorption and Adsorption Processes*; John Wiley & Sons: New York, 1984.
(32) Hill, T. L. In *Thermodynamics of Small Systems, Parts I and II*; Dover Publications: New York, 1994.
(33) Rudzinski, W.; Everett, D. H. In *Adsorption of Gases on Heterogeneous Surfaces*; Academic Press: London, 1992.
(34) Sircar, S. *J. Chem. Soc., Faraday Trans. 1* **1984**, *81*, 1527.
(35) Szepesy, L.; Illes, V. *Acta Chim. Hung. Tomus.* **1963**, *35*, 37.
(36) Szepesy, L.; Illes, V. *Acta Chim. Hung. Tomus.* **1963**, *35*, 53.
(37) Reich, R.; Ziegler, W. T.; Rogers, K. A. *Ind. Eng. Chem. Process Des. Dev.* **1980**, *19*, 336.
(38) Danner, R. P.; Choi, E. C. *Ind. Eng. Chem. Fundam.* **1978**, *17*, 248.
(39) Hyun, S. H.; Danner, R. P. *J. Chem. Eng. Data* **1982**, *27*, 196.
(40) Kaul, B. K. *Ind. Eng. Chem. Res.* **1987**, *26*, 928.
(41) Liu, Y.; Ritter, J. A. *Adsorption* **1998**, *4*, 159.